Polym. Bull. (2010) 64:805–815
DOI 10.1007/s00289-010-0265-2

ORIGINAL PAPER

Effect of conformational asymmetry on the self-assembly of amphiphilic diblock copolymer in selective solvent

Wei Li · Wei Jiang

Received: 20 October 2009 / Revised: 28 February 2010 / Accepted: 7 March 2010 /
Published online: 12 March 2010

Abstract Three dimensional real-space self-consistent field theory is employed to study the effect of conformational asymmetry on the self-assembly of amphiphilic diblock copolymer in selective solvent. The phase diagrams in wide ranges of interaction parameters and conformational asymmetry were obtained in present study. The results indicate that the conformational asymmetry is an important factor that determines the self-assembly of amphiphilic diblock copolymer in solution. The self-assembled morphology changes from sphere to rod, then to vesicle with an increase of the degree of conformational asymmetry. We found that the entropic contribution of the core-forming block is the main reason for this transition.

Keywords Conformational asymmetry · Diblock copolymer · Self-assembly · Selectivity · Self-consistent field theory

Introduction

The importance of conformational asymmetry between different components has been realized in both experimental and theoretical study of many polymeric systems. Foster et al. have shown by means of neutron reflectivity experiments on poly(ethylenepropylene)–poly(ethylethylene) (PEP–PEE) diblock copolymers that the more flexible PEE block segregates preferentially to both air and silicon interfaces [1]. Fredrickson et al. constructed an expression for the free energy of an incompressible binary blend of homopolymers in the vicinity of a hard reflecting

W. Li · W. Jiang (✉)
State Key Laboratory of Polymer Physics and Chemistry, Changchun Institute of Applied Chemistry, Chinese Academy of Sciences, Changchun 130022, People's Republic of China
e-mail: wjiang@ciac.jl.cn

W. Li · W. Jiang
Graduate University of the Chinese Academy of Sciences, Beijing, People's Republic of China

surface. They found if the difference in surface energies is very small, the conformational mismatch in binary polymer blends can drive the conformationally smaller or more flexible species to enrich the surface [2, 3]. Recently, Zhou et al. developed a ternary polymeric system, poly(ethylene-alt-propylene) (PEP)/poly (butylenes oxide) (PBO)/PEP–PBO, to study the complex phase behavior near the bicontinuous microemulsion phase channel. It was found that the bicontinuous microemulsion channel is consistently cut off at low temperature by a hexagonal phase with the more flexible component PBO constructing the core of the cylinders. It is attributed to the dramatic effect of the conformational asymmetry between PEP and PBO [4].

Vavasour and Whitmore defined a single parameter ε to characterize conformational asymmetry of diblock copolymer [5].

$$\varepsilon = \rho_{0B} b_B^2 / \rho_{0A} b_A^2 \tag{1}$$

Here, b is the Kuhn statistical length and ρ_0 is the pure component density. They calculated the phase diagram for $\varepsilon = 0.6$ via self-consistent field theory (SCFT). It was found that the order–disorder boundary to be virtually unaffected by the conformational asymmetry, but all the order–order boundaries to be shifted toward higher A content. Their results were in agreement with the experiment by Bates et al. [6]. This SCF treatment for conformationally asymmetric polymers was subsequently refined by Matsen and Bates [7]. They found that the conformational asymmetry significantly affects the relative stability of the complex phases, e.g., the perforated lamellar phase.

Although there were so many outstanding studies on the effect of conformational asymmetry of polymer melts, little theoretical attention was paid to polymer solution. Larson and Terentjev computed phase diagrams for dilute AB diblock copolymers in poor solvent in the strong segregation limit, transitions from spherical to cylindrical and from cylindrical to bicontinuous phases were observed with the increased conformational asymmetry [8, 9]. On the other hand, the crew-cut micelles formed by amphiphilic block copolymers in selective solvent, which can be used in the fields of drug delivery and nanomaterials, have attracted widespread interests in both experimental and theoretical context since the original work of Eisenberg's group [10–14]. However, the study concerning the effect of conformational asymmetry on the self-assembly of amphiphilic block copolymers in selective solvent has not been reported up to now.

SCFT is a powerful tool to characterize the equilibrium thermodynamical features of polymers [15–21]. Fredrickson and co-workers suggested a new combinatorial screening method in real space [22–24], which a prior assumption about the morphology is not necessary. Using this method, Liang and co-workers investigated the formation of the microstructures assembled by the linear block copolymers in dilute solution [25–27]. Complex micelles were obtained by tailoring the interaction parameters, initial density fluctuation, and polydispersity. Yang and co-workers employed the same method to investigate the aggregate morphologies of amphiphilic linear and star ABC triblock copolymers in dilute solution, and obtained the micelles such as peanut, hamburger, wormlike, and toroidal micelles [28, 29].

In this study, we use the combination screening method based on the real-space implementation of the SCFT to simulate the effect of conformational asymmetry on the self-assembly of an amphiphilic diblock copolymer in dilute solution. The main purpose is to reveal the conformational asymmetry dependence of the self-assembled structure and to explore the origin primarily.

Theoretical method

In this section, we outline the SCFT for a mixture of amphiphilic diblock copolymers with hydrophobic segments A, hydrophilic segments B, and solvent molecules S in volume V. Each copolymer consists of N segments of which a fraction f forms the A block. The volume fraction of copolymer in solution is ϕ. As a result, the volume fractions of segments A, B, and solvent S in the system are $f_A = f\phi$, $f_B = (1-f)\phi$ and $f_S = 1-\phi$, respectively. Each block has an associated Kuhn length $b_\alpha = \sigma_\alpha b$, where b is a reference Kuhn length and α = A, B. We assume that the mixture is incompressible and each segment occupying the same volume ρ_0^{-1}. Thus, we can take the ratio $\beta = b_A/b_B$ to characterize the conformational asymmetry of the diblock copolymer.

For the present system, there are three fields, i.e.:

$$\omega_A(r) = \chi_{AB}N(\phi_B(r) - f_B) + \chi_{AS}N(\phi_S(r) - f_S) + \xi(r) \quad (2)$$

$$\omega_B(r) = \chi_{AB}N(\phi_A(r) - f_A) + \chi_{BS}N(\phi_S(r) - f_S) + \xi(r) \quad (3)$$

$$\omega_S(r) = \chi_{AS}N(\phi_A(r) - f_A) + \chi_{BS}N(\phi_B(r) - f_B) + \xi(r) \quad (4)$$

acting on the A segments, B segments, and solvent molecules, respectively. Here, constant shifts in the fields are introduced in the equations, where $\phi_A(r)$, $\phi_B(r)$, and $\phi_S(r)$are standard dimensionless concentrations of these three respective components, χ_{ij} is the Flory–Huggins interaction parameter between species i and j. A Lagrange multiplier field $\xi(r)$ is used to enforce the incompressibility assumption.

$$\phi_A(r) + \phi_B(r) + \phi_S(r) = 1 \quad (5)$$

In SCFT scheme, the partition function is calculated through solving the modified diffusion equation of $q(r,s)$, which gives the probability of the sth segment fixed at position r. The contour variable s increases from 0 to 1, corresponding from one end of the chain to the other. With the use of a flexible Gaussian chain model, the diffusion equation is

$$\frac{\partial}{\partial s}q_\alpha(r,s) = \sigma_\alpha^2\nabla^2 q_\alpha(r,s) - \omega_\alpha q_\alpha(r,s) \quad (6)$$

The initial condition is $q(r,0) = 1$. Here, ω is ω_A when $0 < s < f$ and ω_B when $f < s < 1$. Similarly, a second distribution function $q'(r,s)$ is also satisfied by Eq. 6 with the initial condition $q'(r,0) = 1$, but in this case ω is ω_B when $0 < s < (1-f)$ and ω_A when $(1-f) < s < 1$. In terms of these two functions, the total partition function for the copolymer molecule is

$$Q_C = \int \mathrm{d}r q(r,s) q'(r,s) \tag{7}$$

As the solvent molecule is treated as a point particle, its partition function is given by the simple expression

$$Q_S = \int \mathrm{d}r \exp\{-\omega_s(r)/N\} \tag{8}$$

The dimensionless concentration of each component is obtained by

$$\phi_A(r) = \frac{\phi V}{Q_C} \int_0^f \mathrm{d}s q(r,s) q'(r,s) \tag{9}$$

$$\phi_B(r) = \frac{\phi V}{Q_C} \int_f^1 \mathrm{d}s q(r,s) q'(r,s) \tag{10}$$

$$\phi_S(r) = \frac{(1-\phi)V}{Q_S} \exp\{-w_s(r)/N\} \tag{11}$$

Once the fields have been self-consistently determined, the free energy of the system which is reduced by $k_B T$ is given by

$$\begin{aligned} F = & -\phi \ln\left(\frac{Q_C}{V}\right) - (1-\phi) N \ln\left(\frac{Q_S}{V}\right) \\ & - \frac{1}{V} \int \mathrm{d}r \{\chi_{AB} N \phi_A(r) \phi_B(r) + \chi_{AS} N \phi_A(r) \phi_S(r) \\ & + \chi_{BS} N \phi_B(r) \phi_S(r) - \omega_A(r) \phi_A(r) - \omega_B(r) \phi_B(r) - \omega_S(r) \phi_S(r) \\ & - \xi(r)[1 - \phi_A(r) - \phi_B(r) - \phi_S(r)]\} \end{aligned} \tag{12}$$

The initial value of ω is constructed by $\omega_j = \sum_{i \neq j} \chi_{ij} N(\phi_i(r) - f_i)$ and $\phi_i(r) - f_i$ satisfies the Gaussian distributions:

$$\begin{aligned} \langle (\phi_i(r) - f_i) \rangle &= 0 \\ \langle (\phi_i(r) - f_i)(\phi_j(r') - f_j) \rangle &= \lambda f_i f_j \delta_{ij} \delta(r - r') \end{aligned} \tag{13}$$

Here, λ characterizes the amplitude of initial density fluctuation.The chemical potential field ω_i can be updated by using the equation

$$\omega_i^{\mathrm{new}}(r) = \omega_i^{\mathrm{old}}(r) + \Delta t (\delta F / \delta \phi_i(r))^*, \tag{14}$$

where $(\delta F / \delta \phi_i(r))^* = \sum_{j \neq i} \chi_{ij} N(\phi_j(r) - f_j(r)) + \xi(r) - \omega_i^{\mathrm{old}}(r)$ as the chemical potential force. The density field $\phi_i(r)$ can be evaluated based on Eqs. 6–11. In this work, the time step Δt was set to be 0.3. Above steps are iterated until the phase patterns are stable and the free energy difference between two iterations is smaller than 10^{-4}, i.e., $\Delta F < 10^{-4}$. Furthermore, to avoid the system locating on metastable states as much as possible, the simulation was reiterated at least 10 times with different random states and random number generator seeds to guarantee that the

phenomena are not accidental. The simulations were carried out on the three dimensional space of a 50^3 cubic lattice with periodic boundary conditions applied. The grid size was set to be 0.35.

Results and discussion

The volume fraction of diblock copolymers in the solution ϕ is chosen to be 0.1. The length of the polymer chain N equals 20 and the length fraction of the hydrophobic block f equals 0.9. The variable $\beta = b_A/b_B$ was defined to characterize the conformational asymmetry of the diblock copolymer. We performed our calculation with the value of β from 1.0 to 1.5, ranging from symmetric to a degree of asymmetry on the limit of experiment accessibility.

It is noted that the resulting aggregate morphologies depend on the amplitude of initial density fluctuation, possibly corresponding to different experimental preparation conditions, such as the rate of addition of nonsolvent to the dilute solution [25]. The larger amplitude of concentration fluctuation should generally leads to the sphere and rod micelle, while vesicles can be formed by a smaller value of amplitude of the concentration fluctuation. The micelle morphologies of amphiphilic diblock copolymer in dilute solution from different values of initial density fluctuation amplitude λ with fixed interaction parameters and conformational asymmetry were shown in Fig. 1. Thus, the same amplitude of initial density fluctuation ($\lambda = 1 \times 10^{-3}$) was used in this simulation to ensure that the obtained morphologies were not affected by the initial condition as it was done for the self-assembly of copolymers in dilute solution in literatures [28–30].

Figure 2 is the simulation result showing the self-assembled morphologies from the amphiphilic diblock copolymer in dilute solution by changing the conformational asymmetry of the copolymer. The Flory–Huggins interaction parameters were fixed, $\chi_{AB}N = 24$, $\chi_{AS}N = 24$, $\chi_{BS}N = -10$. This result indicates that the self-assembled morphology strongly depends on the conformational asymmetry of the copolymer. It tends to change from sphere to rod then to vesicle with the increased conformational asymmetry of the copolymer. During the transition from sphere to

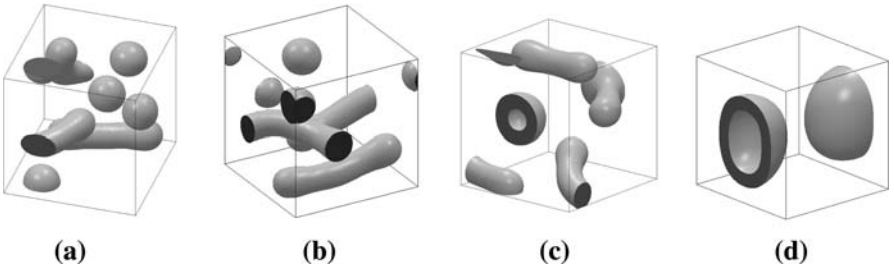

Fig. 1 Micelle morphologies of amphiphilic diblock copolymer in dilute solution from different values of initial density fluctuation amplitude λ with $\chi_{AB}N = 24$, $\chi_{AS}N = 24$, $\chi_{BS}N = -10$, $\beta = 1.0$: **a** $\lambda = 0.1$; **b** $\lambda = 1 \times 10^{-3}$; **c** $\lambda = 1 \times 10^{-6}$; **d** $\lambda = 1 \times 10^{-18}$. The isosurface of the A segment density of the AB diblock copolymer at the value of 0.4 are shown

vesicle, the coexistence of the basic structures is observed, e.g., the mixture of spheres and rods (Fig. 2a–d). Experimental studies have indicated that in general there is coexistence of spheres, rods, vesicles, and more complicated micelles in dilute solution [31, 32]. The micelle change in solution is related to the degree of the stretching of the core-forming chains [10]. From the dimensions of the various structures in Fig. 2, it is of interest to estimate how the degree of the stretching of the core-forming A block changes by measuring the radius of the micelle core. The radius of the micelle core R was shown in Fig. 3. In the case of vesicle, R is half of the wall thickness. The stretching of the A block is greatest in the sphere and decreases as the structure changes from sphere to rod and is smallest in the vesicle. Experimentally, Zhang et al. found that the degree of stretching of the core-forming polystyrene blocks decreases stepwise as the morphology changes from spherical to cylindrical, and to vesicular in solution [33]. Moreover, the radius of the spherical core increases with an increase of the conformational asymmetry of the copolymer, implying a corresponding increase of the degree of stretching of the A block. However, it cannot continue indefinitely as the conformational asymmetry increases. Beyond a certain degree of stretching, the morphology changes from sphere to rod, and eventually to vesicle. The configuration entropy of the polymer with an increase of the conformational asymmetry was calculated to explore the origin of this

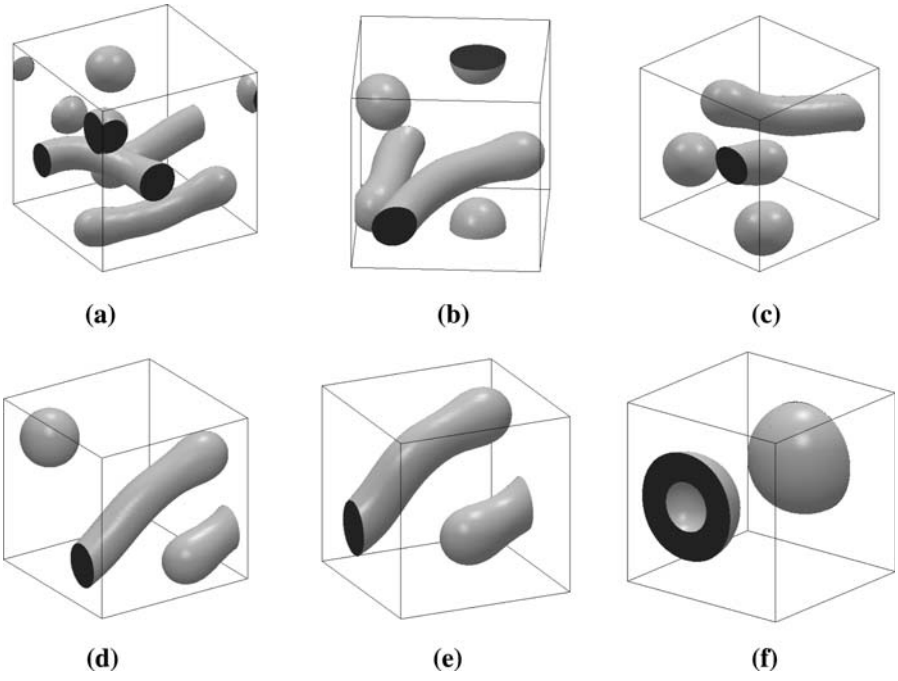

Fig. 2 Micelle morphologies for different conformational asymmetry β **a** $\beta = 1.0$, **b** $\beta = 1.1$, **c** $\beta = 1.2$, **d** $\beta = 1.3$, **e** $\beta = 1.4$, **f** $\beta = 1.5$ with $\chi_{AB}N = 24$, $\chi_{AS}N = 24$, $\chi_{BS}N = -10$. The isosurface of the A segment density of the AB diblock copolymer at the value of 0.4 are shown

transition. The configuration entropy of the polymer S_P was given by the following equation:

$$S_P = \phi \ln\left(\frac{Q_C}{\phi V}\right) + \frac{1}{V}\int dr\,(w_A(r)\phi_A(r) + w_B(r)\phi_B(r)) \tag{15}$$

From Fig. 4, we can see that the entropy of the polymer decrease as β going from 1.0 to 1.3, because of the increased stretching of the core-forming block. To reduce this thermodynamic entropy penalty, the morphology would change toward to the structure with lower degree of stretching, i.e., rod and even vesicle. We can see that the entropy of the polymer rises up when the rods and vesicles formed. As a result, the entropic effect of the core-forming block is the main reason for the morphology change with different conformational asymmetry.

Similar to the self-assembly of block copolymers in bulk, the segregation degree of different blocks has significant influence on the morphology of block copolymers in solution as well. It is important to give a systemic calculation showing the phase diagrams in wide ranges of interaction parameters and conformational asymmetry. Figure 5 is the phase diagram plotted as a function of the Flory–Huggins interaction parameter between hydrophobic segments A and hydrophilic segments B, $\chi_{AB}N$, and conformational asymmetry, β. Other interaction parameters were fixed, $\chi_{AS}N = 24$, $\chi_{BS}N = -10$. The regions for mixture of spheres and rods, rods, mixture of spheres, rods and vesicles, mixture of spheres and vesicles, and vesicles are denoted by SR, R, SRV, SV and V, respectively. It can be found that the transition from spheres to vesicles is general in a wide range of segregation parameters. However, the vesicles were not favored in the strong segregation regions except when the conformational asymmetry is very high. Furthermore, the vesicle regions shift to high conformational asymmetry with an increase of $\chi_{AB}N$. Although increasing the conformational asymmetry can lead to form vesicles, the increased degree of

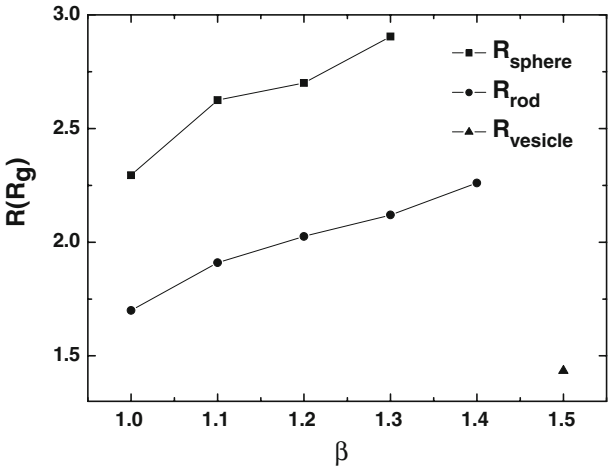

Fig. 3 Radius of the micelle core for sphere, rod, and vesicle with different β for $\chi_{AB}N = 24$, $\chi_{AS}N = 24$, $\chi_{BS}N = -10$. In the case of vesicle, R is half of the wall thickness

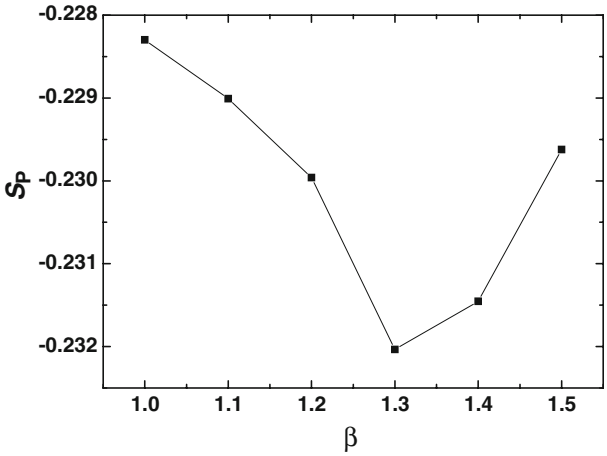

Fig. 4 Configuration entropy of the copolymer with different β for $\chi_{AB}N = 24$, $\chi_{AS}N = 24$, $\chi_{BS}N = -10$

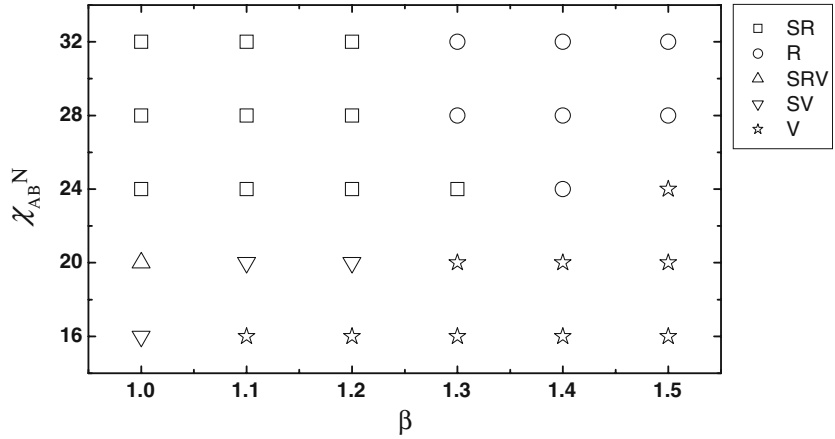

Fig. 5 Phase diagram for amphiphilic diblock copolymer in solution in terms of $\chi_{AB}N$ and β with $\chi_{AS}N = 24$, $\chi_{BS}N = -10$. The regions for mixture of spheres and rods, rods, mixture of spheres, rods and vesicles, mixture of spheres and vesicles, and vesicles are denoted by SR, R, SRV, SV, and V, respectively

segregation has a hindering effect on the stretching of the core-forming block. Thus, the phase diagram would be determined by the two factors balance.

A number of experimental and theoretical studies have been carried out to investigate the influence of the solvent property on the morphology in amphiphilic copolymer solution [34–36]. More recently, Suo et al. found that a strongly selective solvent can make the diblock copolymer self-assembling behavior diverse [37]. However, the study which allows for both the property of the solvent and conformational asymmetry have not been reported up to now. In Fig. 6, we plotted the phase diagram as a function of the Flory–Huggins interaction parameter between

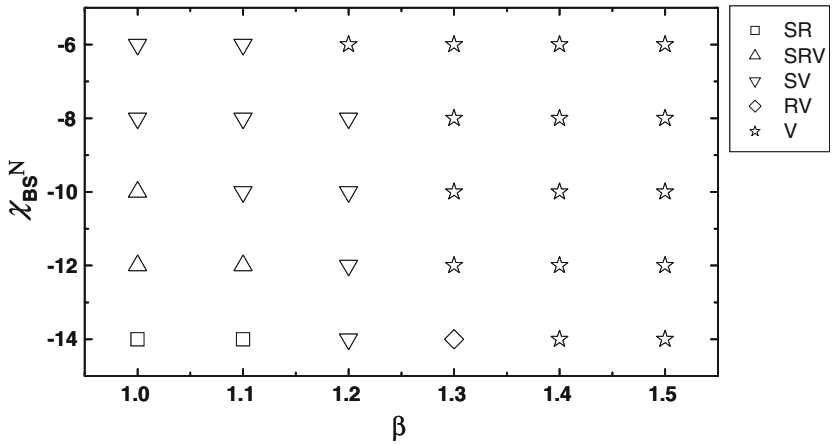

Fig. 6 Phase diagram for amphiphilic diblock copolymer in solution in terms of $\chi_{BS}N$ and β with $\chi_{AS}N = 24$, $\chi_{AB}N = 20$. The regions for mixture of spheres and rods, mixture of spheres, rods and vesicles, mixture of spheres and vesicles, mixture of rods and vesicles and vesicles are denoted by SR, SRV, SV, RV, and V, respectively

hydrophilic segments B and solvent S,$\chi_{BS}N$, and conformational asymmetry, β. Other interaction parameters were fixed, $\chi_{AB}N = 20$, $\chi_{AS}N = 24$. It can be seen that the system undergoes spheres to vesicles phase road with an increase of the conformational asymmetry as mentioned above. The preferred morphology for large asymmetries is also the vesicles. Similar observation was found by Larson and Terentjev in poor solvent in the strong segregation limit. One of their remarkable results is that spherical micelles are not favored for very asymmetric polymers [8]. Moreover, large number of spheres and rods appeared at the low conformational asymmetry when the hydrophilic interaction was enhanced. The degree of the stretching of hydrophilic block B was strengthened with the increased hydrophilic interaction. Thus, the mismatch in the entropic chain stretching penalty between segment A and B was weakened with the increasing of the stretching of hydrophilic block B. Maskos constructed a experimental phase diagram of nanoparticles based on self-assembled amphiphilic poly(1,2-butadiene)-b-poly(ethylene oxide) diblock copolymers (PB-b-PEO) in selective solvent [38]. It was found that the resulting morphology of the nanoparticles in water is shifted to a higher ratio of PB for copolymers containing a PEO-sided carboxy end group (PB_xPEO_y-COOK) as compared to the hydroxyl-terminated block copolymers (PB_xPEO_y-H). It is also because of the increased stretching of the PEO corona chains of diblock copolymers PB_xPEO_y-COOK than copolymers PB_xPEO_y-H.

Conclusion

In summary, we have examined the effect of conformational asymmetry on the phase behavior of diblock copolymer in selective solvent using the 3D real-space SCFT. It turns out that the morphology of the crew-cut micelles formed in the

solution strongly depends on the conformational asymmetry. The self-assembled micelle changes from sphere to rod, then to vesicle to reduce the thermodynamic entropy penalty of the core-forming block. Furthermore, these transitions were found in a wide range of interaction parameters.

Acknowledgments This work was financially supported by the National Natural Science Foundation of China for Major Program (50930001), Creative Research Groups (50621302), Outstanding Young Investigators (50725312), and the National Basic Research Program (2007CB808000) of China.

References

1. Foster MD, Sikka M, Singh N, Bates FS, Satija SK, Majkrzak CF (1992) Structure of symmetric polyolefin block copolymer thin films. J Chem Phys 96:8605–8615
2. Fredrickson GH, Donley JP (1992) Influence of broken conformational symmetry on the surface enrichment of polymer blends. J Chem Phys 97:8941–8946
3. Wu DT, Fredrickson GH, Carton JP (1996) Surface segregation in conformationally asymmetric polymer blends: incompressibility and boundary conditions. J Chem Phys 104:6387–6397
4. Zhou N, Lodge TP, Bates FS (2006) Influence of conformational asymmetry on the phase behavior of ternary homopolymer/block copolymer blends around the bicontinuous microemulsion channel. J Phys Chem B 10:3979–3989
5. Vavasour JD, Whitmore MD (1993) Self-consistent field theory of block copolymers with conformational asymmetry. Macromolecules 26:7070–7075
6. Bates FS, Schulz MF, Khandpur AK, Forster S, Rosedale JH, Almdal K, Mortensen K (1994) Fluctuations, conformational asymmetry and block copolymer phase behaviour. Faraday Discuss 98:7–18
7. Matsen MW, Bates FS (1997) Conformationally asymmetric block copolymers. J Polym Sci B 35:945–952
8. Larson AL, Terentjev EM (2006) Spontaneous curvatures of copolymer interfaces in poor solvents: monolayer morphology. Macromolecules 39:9497–9507
9. Larson AL, Terentjev EM (2006) Spontaneous curvatures of copolymer interfaces in poor solvents: bilayer morphology. Macromolecules 39:9508–9518
10. Zhang L, Eisenberg A (1995) Multiple morphologies of "crew-cut" aggregates of polystyrene-b-poly(acrylic acid) block copolymers. Science 268:1728–1731
11. Zhang L, Eisenberg A (1999) Crew-cut aggregation form self-assembly of blends of polystyrene-b-poly(acrylic acid) block copolymers and homopolystyrene in solution. J Polym Sci B 37:1469–1484
12. Hurtrez G, Dumas P, Riess G (1998) Polystyrene-poly(ethylene oxide) diblock copolymers micelles in water. Polym Bull 40:203–210
13. Zhu JT, Jiang W (2005) Self-assembly of ABC triblock copolymer into giant segmented wormlike micelles in dilute solution. Macromolecules 38:9315–9323
14. Won YY, Davis HT, Bates FS (1999) Giant wormlike rubber micelles. Science 283:960–963
15. Edwards SF (1965) The statistical mechanics of polymers with excluded volume. Proc Phys Soc 85:613–624
16. Helfand E (1975) Theory of inhomogeneous polymers: fundamentals of the Gaussian random-walk model. J Chem Phys 62:999–1005
17. Matsen MW, Schick M (1994) Stable and unstable phases of a diblock copolymer melt. Phys Rev Lett 72:2660–2663
18. Shi AC, Noolandi J, Desai RC (1996) Theory of anisotropic fluctuations in ordered block copolymer phases. Macromolecules 29:6487–6504
19. Noolandi J, Shi AC, Linse P (1996) Theory of phase behavior of poly(oxyethylene)- poly(oxypropylene)-poly(oxyethylene) triblock copolymers in aqueous solutions. Macromolecules 29:5907–5919
20. Müller M, Schmid F (2005) Incorporating fluctuations and dynamics in self-consistent field theories for polymer blends. Adv Polym Sci 85:1–58

21. Daoulas KC, Müller M, de Pablo JJ, Nealey PF, Smith GD (2006) Morphology of multi-component polymer systems: single chain in mean field simulation studies. Soft Matter 2:573–583
22. Drolet F, Fredrickson GH (1999) Combinatorial screening of complex block copolymer assembly with self-consistent field theory. Phys Rev Lett 83:4317–4320
23. Drolet F, Fredrickson GH (2001) Optimizing chain bridging in complex block copolymers. Macromolecules 34:5317–5324
24. Fredrickson GH (2006) The equilibrium theory of inhomogeneous polymers. Clarendon Press, Oxford
25. He XH, Liang HJ, Huang L, Pan CY (2004) Complex microstructures of amphiphilic diblock copolymer in dilute solution. J Phys Chem B 108:1731–1735
26. Zhu JT, Jiang Y, Liang HJ, Jiang W (2005) Self-assembly of ABA amphiphilic triblock copolymers into vesicles in dilute solution. J Phys Chem B 109:8619–8625
27. Jiang Y, Zhu JT, Jiang W, Liang HJ (2005) Cornucopian cylindrical aggregate morphologies from self-assembly of amphiphilic triblock copolymer in selective media. J Phys Chem B 109:21549–21555
28. Wang R, Tang P, Qiu F, Yang YL (2005) Aggregate morphologies of amphiphilic ABC triblock copolymer in dilute solution using self-consistent field theory. J Phys Chem B 109:17120–17127
29. Ma JW, Li X, Tang P, Yang YL (2007) Self-assembly of amphiphilic ABC star triblock copolymers and their blends with AB diblock copolymers in solution: self-consistent field theory simulations. J Phys Chem B 111:1552–1558
30. Zhang LS, Lin JP, Lin SL (2007) Aggregate morphologies of amphiphilic graft copolymers in dilute solution studied by self-consistent field theory. J Phys Chem B 111:9209–9217
31. Jain S, Bates FS (2003) On the origins of morphological complexity in block copolymer surfactants. Science 300:460–464
32. Bang J, Jain S, Li Z, Lodge TP, Pedersen JS, Kesselman E, Talmon Y (2006) Sphere, cylinder, and vesicle nanoaggregates in poly(styrene-b-isoprene) diblock copolymer solutions. Macromolecules 39:1199–1208
33. Zhang L, Eisenberg A (1998) Formation of crew-cut aggregates of various morphologies from amphiphilic block copolymers in solution. Polym Adv Technol 9:677–699
34. Yu Y, Eisenberg A (1997) Control of morphology through polymer-solvent interactions in crew-cut aggregates of amphiphilic block copolymers. J Am Chem Soc 19:8383–8384
35. Yu Y, Zhang L, Eisenberg A (1998) Morphogenic effect of solvent on crew-cut aggregates of amphiphilic diblock copolymers. Macromolecules 31:1144–1154
36. Du HB, Zhu JT, Jiang W (2007) Study of controllable aggregation morphology of ABA amphiphilic triblock copolymer in dilute solution by changing the solvent property. J Phys Chem B 111:1938–1945
37. Suo TC, Yan DD, Yang S, Shi AC (2009) A theoretical study of phase behaviors for diblock copolymers in selective solvents. Macromolecules 42:6791–6798
38. Maskos M (2006) Influence of the solvent and the end groups on the morphology of cross-linked amphiphilic poly(1, 2-butadiene)-b-poly(ethylene oxide). Polymer 47:1172–1178